Geophys. J. Int. (2007) doi: 10.1111/j.1365-246X.2007.03494.x

New constraints on relative motion between the Pacific Plate and Baja California microplate (Mexico) from GPS measurements

C. Plattner,[1] R. Malservisi,[1] T. H. Dixon,[2] P. LaFemina,[2,*] G. F. Sella,[3] J. Fletcher[4] and F. Suarez-Vidal[4]

[1]*Sektion Geophysik der Ludwig-Maximilians Universität, Theresienstr.* 41, 80333 *München, Germany. E-mail: plattner@geophysik.uni-muenchen.de*
[2]*Rosenstiel School of Marine and Atmospheric Sciences, University of Miami,* 4600 *Rickenbacker Causeway, Miami,* FL 33149*, USA*
[3]*National Geodetic Survey, NOAA,* 1315 *East-West Highway, Silver Spring, MD* 20910*, USA*
[4]*Centro de Investigacion Cientifica y Educacion Superior de Ensenada, Km.* 107 *Carretera Tijuana Ensenada, Ensenada* BC 2732, *Mexico*

Accepted 2007 May 14. Received 2007 May 14; in original form 2007 March 13

SUMMARY

We present a new surface velocity field for Baja California using GPS data to test the rigidity of this microplate, calculate its motion in a global reference frame, determine its relative motion with respect to the North American and the Pacific plates, and compare those results to our estimate for Pacific–North America motion. Determination of Pacific Plate motion is improved by the inclusion of four sites from the South Pacific Sea Level and Climate Monitoring Project. These analyses reveal that Baja California moves as a quasi-rigid block but at a slower rate in the same direction, as the Pacific Plate relative to North America. This is consistent with seismic activity along the western edge of Baja California (the Baja California shear zone), and may reflect resistance to motion of the eastern edge of the Pacific Plate caused by the 'big bend' of the San Andreas fault and the Transverse Ranges in southern California.

Key words: geodesy, global positioning system (GPS), plate tectonics, tectonics.

INTRODUCTION

Plate rigidity is a key assumption in plate tectonics. While this assumption works well for plate interiors, plate boundaries can include a broad region of deformation and the development of multiple blocks or 'microplates'. This is particularly true for the Pacific–North American Plate boundary (e.g. Atwater & Stock 1988). Identifying these rigid blocks provides important kinematic boundary conditions for tectonic studies of western North America.

Constraints on North America–Pacific Plate motion are also important for kinematic tectonic studies of western North America and parts of the circum-Pacific region. Models of this motion on geological timescales (e.g. DeMets *et al.* 1990, 1994) may use magnetic anomalies from the spreading centre in the southern Gulf of California. However, evidence is accumulating that Baja California's motion is distinct from that of the Pacific Plate (Fig. 1) and thus behaves as a separate block or microplate (Dixon *et al.* 2000b; Fletcher & Munguia 2000; Gonzalez-Garcia *et al.* 2003; Michaud *et al.* 2004). Here we use new GPS data to quantify current North America–Pacific Plate motion and investigate coupling and rigidity of Baja California and the Pacific Plate.

*Now at: Pennslyvania State University, University Park, PA 16802, USA.

Data analysis

For the Pacific Plate we use only continuous GPS (CGPS) with time-series longer than 3 yr, giving time-series durations from 3 to 10 yr (Table 1). Compared to previous studies of Pacific Plate motion we add four new sites from the South Pacific Sea Level and Climate Monitoring Project (SPSLCMP) improving kinematic constraints in the central and western Pacific. To reduce the uncertainty in the time-series of GUAX on Guadalupe Island, we added episodic GPS (EGPS) data from GAIR through a vector tie (Sella *et al*. 2002), which extends the time-series back to 1993. The uncertainty of this new time-series, here called GUAZ, is reduced by 40 per cent, while the velocity changes only by 0.1 mm yr^{-1} in all three components.

Thirty-two of 33 GPS stations in Baja California are episodic GPS (EGPS) sites. We use EGPS data from sites with at least three occupation episodes of two and more 24 hr days and a minimum total time span of 6 yr since 1993. We did not use data from before 1993 due to incomplete orbit information.

All data were processed using GIPSY/OASIS II, Release 5.0 software and non-fiducial satellite orbit and clock files provided by the Jet Propulsion Laboratory (Zumberge *et al.* 1997). The data analysis follows Sella *et al.* (2002), but the daily solutions are aligned to IGb00 (Ray *et al.* 2004). The velocity and its uncertainty for each site are then calculated by linear regression. Outliers with an offset of more than three times the formal error are not considered in

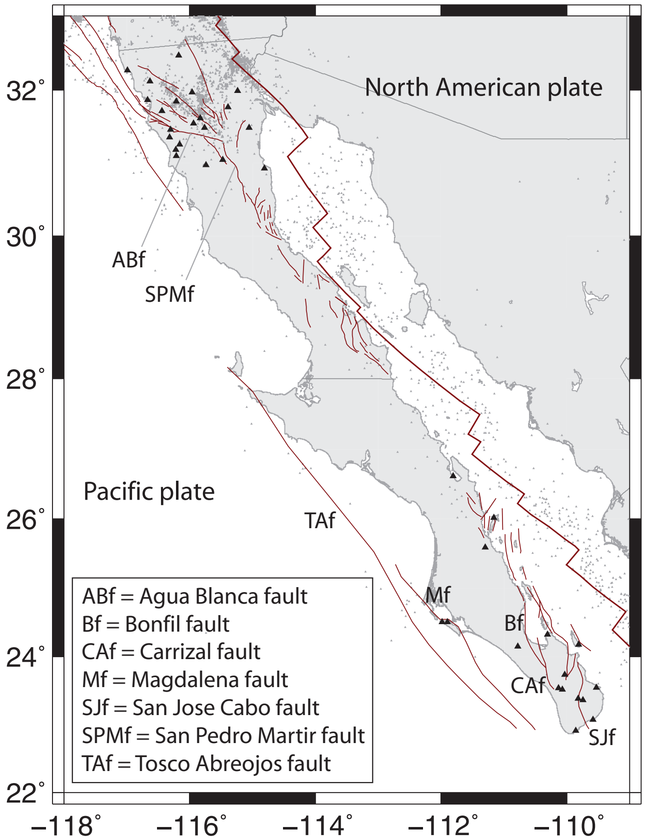

Figure 1. Baja California, Mexico: Faults above latitude 28 from Instituto Nacional Estadistica Geografia e Informatica de Mexico and Dixon *et al.* (2002), faults south of latitude 28 by Paul Umhoefer (personal communication, 2006) and Michaud *et al*. (2004). Epicentres from National Earthquake Center Information (1973 to present). The geologically defined rigid block is outlined by Agua Blanca fault (ABf), San Pedro Martir fault (SPMf), San Jose del Cabo fault (SJf), Bonfil fault (Bf) and Carrizal fault (CAf), Tosco Abreojos fault (TAf) and Magdalena fault (Maf).

the regression. Velocity uncertainties are calculated following Mao *et al.* (1999) and Dixon *et al.* (2000a).

We calculate the stable plate reference frames for Pacific and Baja California by the best fitting Euler vector (Minster *et al.* 1974; Ward 1990), testing for plate rigidity by comparing velocity residuals to uncertainties. Using the stable North America reference frame of Sella *et al.* (2006) we calculate its relative plate motion with the Pacific Plate and Baja California microplate.

Stable Pacific Plate reference frame

Using standard geological criteria for the definition of a stable plate (e.g. Sella *et al.* 2002) we initially identified 21 CGPS sites on the Pacific Plate interior. We excluded FALE due to its location in a Subduction-Transform Edge Propagator (STEP) region (Govers & Wortel 2005). FARB, KOKB, NAUR, PAMA, TAHI and UP01 are known to have technical problems or large uncertainties and are, therefore, excluded. We use only one station from the Hawaiian Islands to avoid an overconstraint; the station importance (Minster *et al.* 1974) would sum up to 48 per cent. We choose KOK1 as it is located furthest from volcanic activity. However, we include all Hawaiian Island stations to compare residuals with respect to the stable Pacific Plate.

As the stable Pacific Plate reference frame is based upon a limited number of GPS stations we test its sensitivity to each GPS station. Using a jackknife method we compute 11 rotation poles from the data set of 11 GPS stations (Table 1), leaving out one station at a time. We compare the rotation pole locations and the corresponding average residual motion within the Pacific Plate. For every model we apply the F-test (Stein & Gordon 1984) to test whether we obtain significant improvement. We recognize the limitations of these tests, in the sense that our sample size is small, and the tests assume normal distribution. While the 2-D-error ellipses for all rotation poles overlap at 95 per cent confidence, however, at the level of one standard error, the solutions are sensitive to exclusion of stations GUAZ and CHAT (Fig. 2, Table 2). The F-test implies a significant improvement in the definition of the Pacific Euler vector for the

Table 1. GPS data used for the computation of Pacific Euler vector and their residual rate.

				IGb00				Residual to PA1[c]			PA1
Site id[a]	Lon. (°E)	Lat. (°N)	ΔT (yr)	Ve (mm yr^{-1})	σ Ve[b] (mm yr^{-1})	Vn (mm yr^{-1})	σ Vn[b] (mm yr^{-1})	Rate (mm yr^{-1})	σ[b] rate (mm yr^{-1})	Azi. (°)[d]	Importance (per cent)
chat[1]	−176.57	−43.96	10	−41.2	0.3	32.3	0.3	1.0	0.5	78	–
CKIS[2]	−159.80	−21.20	4	−63.5	0.8	33.8	0.5	0.4	0.7	−46	13
guaz[4]	−118.29	28.88	12	−47.7	0.3	23.4	0.3	2.0	0.6	149	–
hnlc[1]	−157.86	21.30	5	−63.6	0.8	33.8	0.6	0.9	0.9	−71	–
KIRI[2]	172.92	1.35	3	−67.10	1.1	30.7	0.6	1.4	1.0	50	8
KOK1[1]	−159.76	21.98	7	−63.0	0.6	33.8	0.4	0.3	0.5	−22	21
KWJ1	167.73	8.72	6	−69.7	0.7	27.7	0.4	0.6	0.5	176	10
MARC[3]	153.98	24.29	5	−73.3	1.4	21.5	1.2	2.3	1.4	−138	5
maui[1]	−156.26	20.71	7	−63.3	0.4	32.8	0.3	0.9	0.4	−142	–
mkea[1]	−155.46	19.80	9	−63.7	0.4	33.4	0.3	0.7	0.5	−96	–
POHN[2]	158.21	6.96	4	−70.2	1.3	26.5	0.8	1.6	0.9	−7	7
THTI[1]	−149.61	−17.58	7	−66.6	0.8	32.6	0.4	0.5	0.6	−159	20
TRUK[3]	151.89	7.45	4	−72.0	1.6	22.5	0.9	1.5	1.6	−83	6
TUVA[2]	179.20	−8.53	4	−64.2	0.9	31.2	0.5	1.1	1.0	97	10

[a]Only upper case sites are used to compute the Pacific Euler vector. [1]IGS, [2]SPSLCMP, [3]WING, [4]SCEC time-series has been tied using guax and gair.
[b]Uncertainties are 1σ.
[c]Velocity after removing rigid motion of the Pacific Plate (PA1) from the IGb00 velocities at each site. See Table 2 for angular velocity.
[d]Azimuth is the angle of the rate residual in degrees clockwise from North.

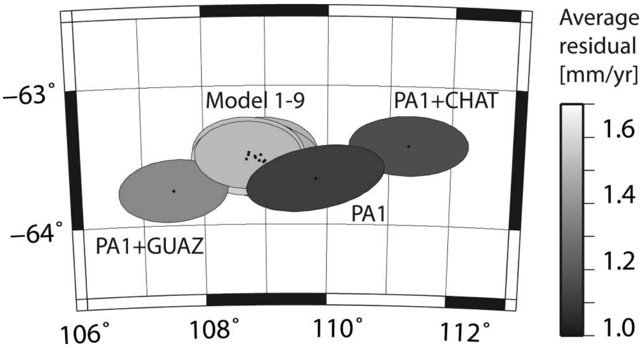

Figure 2. Stability of location of Pacific-IGb00 pole of rotation. Using 10 out of 11 stations we compute 11 rotation poles, leaving out one station at a time. The rotation pole shows increased sensitivity to GUAZ and CHAT. We exclude GUAZ and CHAT and use nine stations (Table 1) to obtain our best-fitting pole of rotation. All rotation pole error ellipses are colour coded by the average residual motion, calculated from of the 11 stations plus HNLC, MKEA and MAUI. For visibility only the 1σ error ellipses showing the 2-D-error are shown.

exclusion of each and both stations. This can be explained by the geographic location of GUAZ and CHAT and their resulting relative importance that varies between 26–33 per cent for CHAT and 32–38 per cent for GUAZ. The residual velocities of GUAZ and CHAT with respect to the Pacific Plate Euler vectors are close to the limit of the 95 per cent confidence interval error ellipse for 9 of the 11 models. In the model for which GUAZ was excluded we also obtain the largest residual for GUAZ (2.6 ± 0.6 mm yr^{-1}), while CHAT shows a near perfect fit (0.4 ± 0.4 mm yr^{-1}). Stations on the Hawaiian Islands, TUVA, MARC, and TRUK show low residuals. In the model for which CHAT is excluded, the residual of CHAT increases to 1.9 ± 0.5 mm yr^{-1}, while GUAZ is fit better (0.6 ± 0.4 mm yr^{-1}), together with good fits at THTI, CKIS, KIRI, and POHN. In general, these results are consistent with a rigid Pacific Plate, within limits defined by our data uncertainty, ∼2 mm yr^{-1}.

Our best-fitting Pacific Plate Euler vector PA1 is based on nine stations, excludes GUAZ and CHAT, and has a reduced χ^2 of 1.00 (Tables 1 and 2). The station importance for this solution varies between 5 and 21 per cent (Table 1). The average residual velocity of the 14 stations on the interior of the Pacific Plate is 1.1 mm yr^{-1}. GUAZ shows significant residual motion, while CHAT and MAUI have residual velocities close to the error limit (Fig. 3, Table 1).

Rigidity of the Baja California microplate

Geological observations suggest rigid block behaviour for Baja California (e.g. Gastil *et al.* 1975; Suarez-Vidal *et al.* 1991; Umhoefer & Dorsey 1997; Umhoefer 2000). The northern and southern ends of the peninsula are cut by several faults, but there is no apparent deformation along the main body of the peninsular batholith. We calculate a Baja California Euler vector using GPS data from stations located within the geologically rigid block

Table 2. Pacific, North American and Baja California Euler vectors.

Rotation pole[a]	Lon. (°E)	Lat. (°N)	Omega (deg Myr^{-1})	σmax σmin[a]	Azi. (°)[b]	χ/ d.o.f.
Pacific Plate–IGb00						
PA1 (This study nine stations[c]) – IGb00	109.81	−63.67	0.681 ± 0.003	0.6 0.3	79	1.00
PA1 + GUAZ (10 stations)–IGb00	107.50	−63.75	0.677 ± 0.003	0.4 0.3	86	1.62
PA1 + CHAT (10 stations)–IGb00	111.31	−63.43	0.679 ± 0.003	0.5 0.2	90	1.47
North America–IGb00						
Sella *et al.* 2006	−83.82	−5.66	0.195 ± 0.001	0.4 0.1	−1	
North America–Pacific (geodetic)						
Sella *et al.* 2006 – PA1	−75.89	50.16	0.769 ± 0.004	0.5 0.3	−85	
Sella *et al.* 2006 – PA1 + GUAZ	−77.32	50.11	0.766 ± 0.004	0.4 0.2	−87	
Sella *et al.* 2006 – PA1 + CHAT	−74.95	49.98	0.7680 ± 0.004	0.5 0.2	77	
Beavan *et al.* 2002	−75.04	50.26	0.773 ± 0.005	0.4 0.2	94	
DeMets & Dixon 1999	−73.70	51.50	0.765 ± 0.016	2.0 1.0	−85	
Gonzalez-Garcia *et al.* 2003	−77.01	49.89	0.766 ± 0.007	0.3 0.2	70	
Sella *et al.* 2002	−72.11	50.38	0.755 ± 0.004	0.6 0.4	−79	
North America–Pacific (geological)						
NUVEL-1A (DeMets 1994)	−78.2	48.7	0.749 ± 0.012	1.3 1.2	−61	
Baja California–IGb00						
BAC1[d]–IGb00	106.63	−64.73	0.637 ± 0.034	4.4 0.4	−53	3.50
North America–Baja California						
Sella *et al.* 2006 – BAC1	−78.11	50.16	0.725 ± 0.039	3.14 0.4	62	

Note: The first plate rotates counter-clockwise relative to the second plate around the stated rotation pole.
[a]Lengths in degrees of the semi-major axes sig maj and semi-minor axes sig min of the 1σ pole error ellipse. Both axes are derived from a 2-D error distribution.
[b]Azimuth of the semi-major ellipse axis in degrees clockwise from north.
[c]List of nine sites used see Table 1.
[d]List of 10 sites used see Table 3.
Angular velocity of PA1 relative to IGb00 in cartesian coordinates with covariance matrix. The X, Y, Z axes are parallel to (0°N,0°E), (0°N, 90°E), and (90°N), respectively.
Omega (10^{-3} rads Myr^{-1}): omegaX = −1.8186589 omegaY = 4.9377246 omegaZ = −10.6312041.
Covariance matrix (10^{-6} rads Myr^{-}): xx = 0.0064931 xy = 0.0006229 xz = −0.0002533 yy = 0.0010012 yz = −0.0000000 zz = 0.0026199.
Angular velocity of BAC1 relative to IGb00 in cartesian coordinates with covariance matrix:
Omega (10^{-3} rads Myr^{-1}): omegaX = −1.3575097 omegaY = 4.5444985 omegaZ = −10.0461015.
Covariance matrix (10^{-6} rads Myr^{-}): xx = 0.0865653 xy = 0.1960590 xz = −0.1088797 yy = 0.4638906 yz = −0.2558797 zz = 0.1455125.

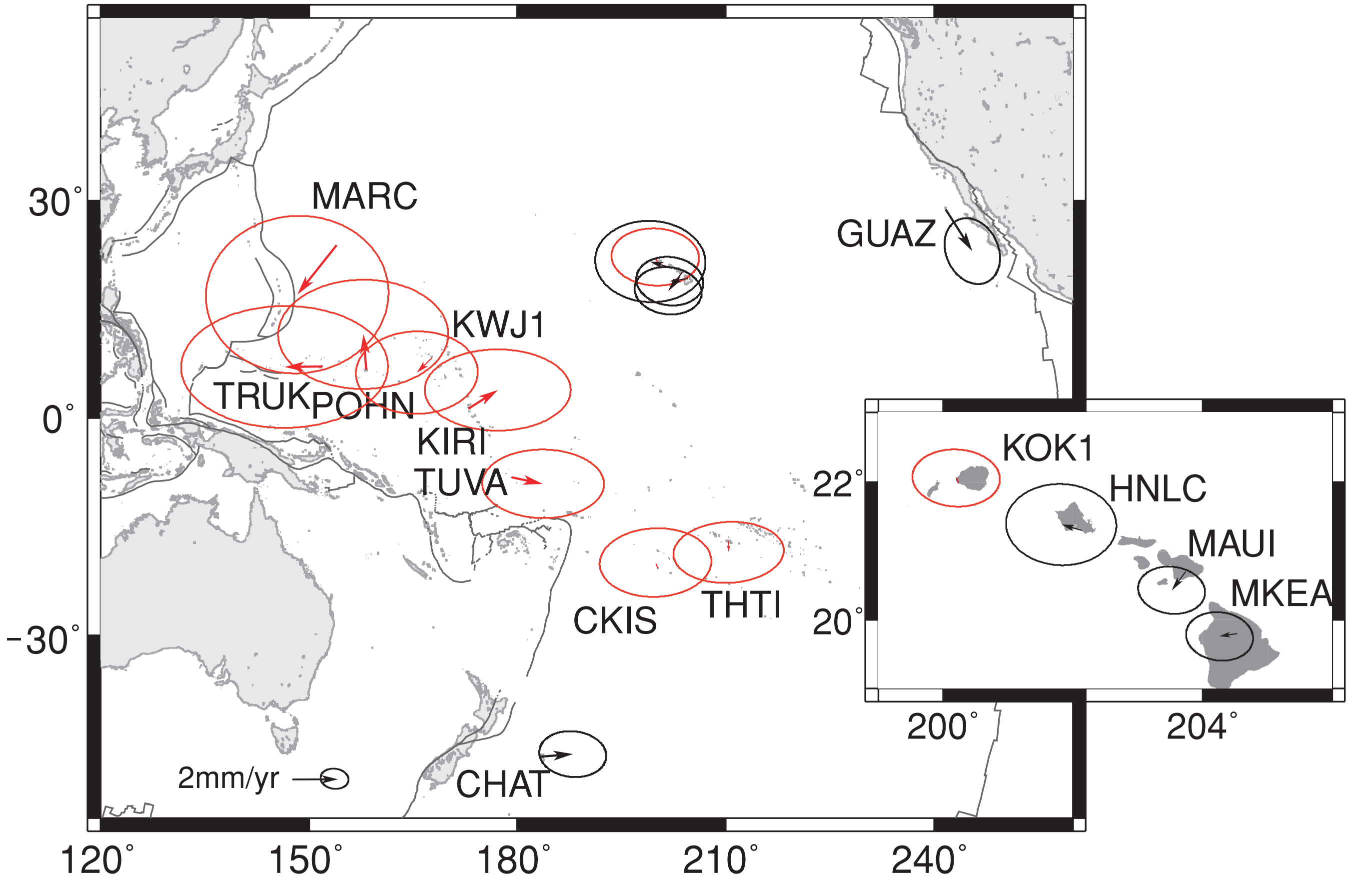

Figure 3. Residual velocity with respect to best fitting Pacific Plate Euler vector (Table 1). Stations used for the computation of the Euler vector are shown in red. Error ellipses indicate 95 per cent confidence interval, to distinguish significant residual motion. Fault and Plate boundaries from the same sources of Fig. 1.

(Table 3). The Agua Blanca fault along with the San Pedro Martir fault marks the northern boundary of the block (Fig. 1). The southern block boundary includes the Bonfil fault, the Carrizal fault and the San Jose Cabo fault (Fig. 1). We exclude GPS stations LOSA and SPMX, located close to the Agua Blanca fault and San Pedro Martir fault, respectively, and possibly influenced by strain accumulation (Dixon *et al.* 2002). The shape of the Baja California peninsula poses problems to an Euler vector calculation due to its limited east–west extent, reflected in the orientation of the ellipsoid describing its uncertainty (Table 2). The best fitting Euler vector has a reduced χ^2 misfit of 3.5. All residual rates within the geologically rigid block are within uncertainties at 95 per cent confidence (Fig. 4; Table 3). However, the azimuths of the residuals do not appear to be randomly oriented, as the northern network has its residual motion directed towards the south and vice versa (Fig. 4). For the northern network the mean residual rate is 1.7 ± 0.8; for the south it is 1.3 ± 0.8 mm yr^{-1}. This apparent convergence may reflect data uncertainty, or perhaps internal deformation of the block. In the latter case the average shortening strain rate between the two networks is $\sim 1 \times 10^{-16}$ s^{-1}. Additional EGPS data from Baja California will be required to distinguish between these hypotheses.

We tested for the effect of elastic strain accumulation at the edges of the microplate using the block model code DEFNODE (McCaffrey 2002). We found that stations LOSA and SPMX are affected by strain accumulation when assuming a standard locking depth of the block bounding faults between 10 and 20 km. All other stations within the geologically rigid block are unaffected by strain accumulation. Therefore, we believe our Baja California Euler vector adequately represents the rigid microplate motion within the defined uncertainty limits.

We find that sites AGUA, CARD, TOSA and CABO in the southern network move with very similar rate and direction with respect to rigid Baja California. Therefore, our geodetic measurements cannot resolve motion across the Carrizal fault, which has sometimes been described to cut through the peninsula (e.g. Hausback 1984). This suggests that the southwestern tip of the peninsula belongs to the rigid microplate (Fig. 4). Other stations in the southern tip of Baja California may represent the motion of smaller blocks that are bounded by active normal faults. This is compatible with the recent geological observations of Busch *et al.* (2006).

Pacific – Baja California motion

We tested the significance of a separate Baja California microplate compared to a larger Pacific Plate including Baja California by applying the F-test (Stein & Gordon 1984). Baja California acts as a separate microplate with 99 per cent confidence. Since Guadalupe Island shows significant residual motion with respect to our Pacific Euler vector PA1 we also tested the possibility that it may be part of the Baja California microplate. The F-test indicates that this is not the case at 99 per cent confidence, implying that the western border of the Baja California microplate lies east of Guadalupe Island.

Table 3. Velocity of GPS stations in Baja California and residual motion with respect to the stable Pacific Plate PA1.[a]

			IGb00				Residual to PA 1			Residual to BAC1		
Site id	Lon (°E)	Lat. (°N)	*Ve* (mm yr^{-1})	σ *Ve* (mm yr^{-1})	*Vn* (mm yr^{-1})	σ *Vn* (mm yr^{-1})	Rate (mm yr^{-1})	σ rate (mm yr^{-1})	Azi. (°)	Rate (mm yr^{-1})	σ rate (mm yr^{-1})	Azi. (°)
AGUA	−111.30	25.59	−48.4	0.3	19.6	0.6	3.2	0.7	141	1.3	0.6	−39
ancn	−110.03	23.74	−51.0	1.7	18.6	0.7	3.1	1.0	163	2.1	1.7	−75
blnd	−110.31	24.33	−48.7	0.7	20.2	0.7	3.1	0.8	118	2.0	0.8	−5
burr	−110.07	23.52	−48.7	1.3	19.8	0.8	3.8	1.3	117	1.8	0.1	15
CABO	−109.86	22.92	−50.4	0.7	18.6	0.5	3.6	0.7	143	1.0	0.7	−51
CADG	−116.32	31.36	−41.6	0.8	19.5	0.7	6.4	0.9	137	2.0	0.9	123
CARD	−110.78	24.15	−49.3	1.3	19.7	0.5	3.2	1.1	133	1.5	0.8	−23
cice	−116.67	31.87	−40.2	0.9	17.4	0.8	8.8	1.0	142	4.3	0.9	141
COLO	−116.21	31.10	−42.3	0.8	19.8	0.7	5.9	0.9	138	1.4	0.9	122
CONC	−111.81	26.62	−45.7	1.1	18.7	0.8	5.3	1.1	133	1.1	1.2	95
ecer	−109.81	24.18	−48.3	0.9	20.4	1.0	3.3	1.0	108	2.5	1.1	6
elal	−116.21	31.85	−39.8	0.7	20.4	1.0	6.8	0.9	123	3.1	0.9	93
elch	−115.05	31.49	−37.0	0.6	16.2	0.5	11.4	0.7	131	7.1	0.7	123
elco	−116.17	32.47	−37.5	0.7	17.1	0.9	10.2	0.9	134	5.9	0.9	126
elja	−115.76	31.49	−39.9	0.8	18.4	0.6	8.1	0.8	134	3.8	0.9	122
elmo	−116.99	32.27	−39.8	1.1	18.1	1.0	8.4	1.1	139	3.9	1.1	135
emir	−109.74	23.37	−51.3	1.0	17.7	0.6	3.8	0.8	167	2.1	1.1	−89
filo	−116.44	31.72	−40.9	1.5	21.3	1.2	5.6	1.5	122	2.2	1.6	73
inde	−115.94	31.55	−39.4	1.0	18.4	0.6	8.5	1.0	132	4.2	1.0	119
lagh	−115.96	31.97	−37.8	0.9	18.1	0.7	9.6	0.9	128	5.4	1.0	116
losa	−116.3	31.46	−41.6	0.9	19.6	0.6	6.3	0.9	137	1.9	0.9	122
mayo	−115.24	31.99	−35.7	1.7	15.1	0.9	12.8	1.5	133	8.5	1.5	127
MELR[a]	−115.74	30.98	−42.5	0.6	19.7	0.8	5.7	0.9	139	1.3	0.8	123
rive	−109.53	23.55	−49.5	1.0	20.0	0.5	2.8	1.0	118	2.2	0.7	−11
rlov	−116.63	32.12	−39.2	0.9	18.4	0.8	8.5	1.0	134	4.2	1.0	124
SAIS	−116.22	31.19	−41.7	0.9	19.5	0.6	6.4	0.9	137	2.0	0.9	121
sald	−115.39	31.77	−36.6	1.0	16.5	0.9	11.4	1.1	130	7.2	1.1	121
sfai	−114.81	30.93	−42.8	1.0	16.1	0.7	8.2	0.9	156	4.0	0.8	171
SLRE	−116.16	31.26	−42.4	0.7	19.0	0.5	6.4	0.7	141	1.9	0.7	134
sm01	−115.83	31.62	−41.0	0.9	17.9	1.3	7.7	1.3	143	3.2	1.2	142
spmx	−115.47	31.05	−43.5	0.6	18.3	0.5	6.2	0.7	155	2.0	0.7	−179
TOSA	−110.13	23.54	−49.6	0.7	19.5	0.6	3.2	0.8	130	1.5	0.7	−17
wmar	−111.98	24.51	−50.0	1.4	21.1	1.0	2.0	1.3	131	2.6	1.2	−32

[a]Column headings are analogous to Table 1.

The magnitude of relative motion of Baja California with respect to the Pacific Plate depends on the chosen stable Pacific Plate reference frame. The relative motion increases when using PA1 + CHAT, while it decreases when using PA1 + GUAZ, with a range of difference of 1.8 mm yr^{-1} for the mean relative motion. However, all models lead to significant relative motion of the Baja California microplate with respect to the Pacific Plate at 95 per cent confidence interval. In the following we use model PA1.

Except for WMAR, all the EGPS velocities in Baja California relative to the stable Pacific Plate are significant at 95 per cent confidence interval (Table 3; Figs 5a and b). On the rigid microplate the average velocity with respect to the Pacific Plate is 4.9 mm yr^{-1}, ranging from 3.2 ± 0.7 (AGUA) to 6.4 ± 0.9 mm yr^{-1} (CADG). The average rate of the northern network (CADG, COLO, LOSA; MELR; SAIS, SLRE) is 6.2 mm yr^{-1}. In the southern network (AGUA, CABO, CARD and TOSA) the average rate is 3.7 mm yr^{-1}. Outside the rigid microplate, deformation of parts of the plate boundary zone can be observed. The northern part of the peninsula shows an increase of velocity from west to east, approaching the North America–Baja California boundary, that is, the San Andreas/Gulf of California system. The velocity reaches 12.8 ± 1.5 mm at MAYO, indicating significant strain accumulation along the northern faults (Fig. 5a). In the southern part of the peninsula no such pattern is observed. West of the peninsula, station WMAR, located on Isla Margarita, shows a velocity with respect to the Pacific Plate that is zero within uncertainty (Fig. 5b).

North America–Pacific motion

The precision of the geodetic estimates of NA-Pacific motion has improved with time, as more stations become available and GPS time-series become longer (Argus & Heflin 1995; Larson *et al.* 1997; DeMets & Dixon 1999; Freymueller *et al.* 1999; Beavan *et al.* 2002; Sella *et al.* 2002; Gonzales-Garcia *et al.* 2003). Our result for NA-PA1 together with previous results is listed in Table 2, and illustrated in Fig. 6.

We obtain a shift in the location of the North America–Pacific pole of rotation (Table 2) when we use PA1+CHAT or PA1+GUAZ instead of PA1 for the Pacific Plate. The results are comparable to the difference in location of the North America–Pacific pole of rotation from Beavan *et al.* (2002) compared to the one of Gonzalez-Garcia *et al.* (2003). This may be because Beavan *et al.* (2002) use CHAT and EGPS data from the Campbell Plateau (analogous to PA1 + CHAT), while Gonzalez-Garcia *et al.* (2003) use one CGPS and three EGPS stations from Guadalupe Island (analogous to PA1 + GUAZ).

Comparing our Euler vectors we see that the North America–Pacific rotation rate is significantly faster than North America–Baja

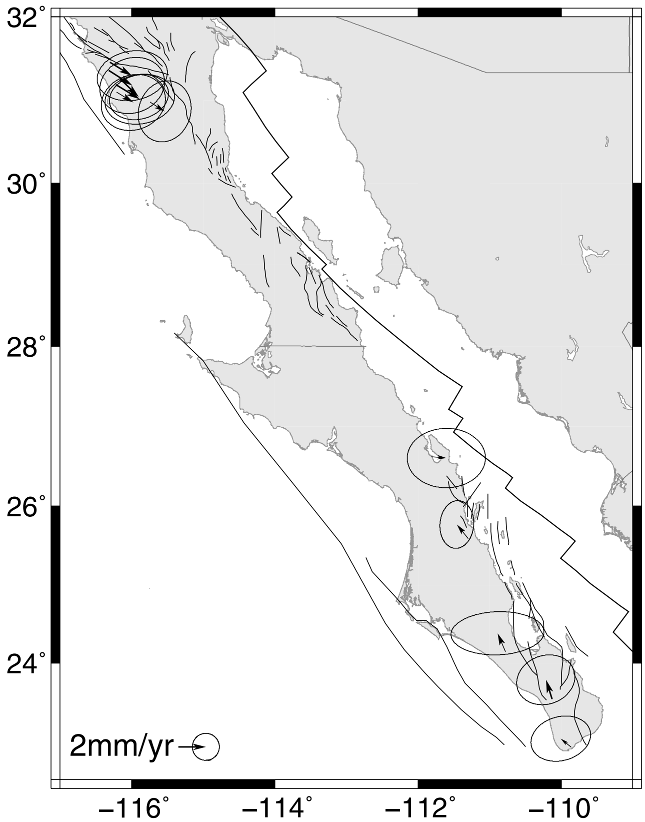

Figure 4. Stations on the Baja California microplate: residual motion with respect to Baja California Euler vector (Table 1). Error ellipses indicate 95 per cent confidence interval.

California. At the location 23.5°N, 108.5°E, at the spreading centre in the Gulf of California (DeMets 1995), we calculate North America–Pacific motion to be 51.1 ± 0.4 mm yr^{-1} at an azimuth of 125 ± 1° clockwise from north. Relative motion between North America and Baja California at the same location is only 46.8 ± 0.4 mm yr^{-1}, 124 ± 1° clockwise from north. This leaves a residual motion of 4.3 ± 0.8 mm yr^{-1} between Baja California and the Pacific Plate. The negligible difference in azimuth, which is also indicated by the proximity of the two Euler poles, shows that Baja California is moving in approximately the same direction as the Pacific Plate with respect to North America.

Along the Gulf of California, the geodetic rate for North America–Baja California derived from our Euler vector decreases from south to north, 46.8 ± 0.4 mm yr^{-1} (23.5°N, 108°W) to 43.1 ± 0.4 mm yr^{-1} at the Colorado River delta (31.8°N, −114.5°W).

A key constraint for the North America–Pacific Euler vector magnitude in NUVEL-1A (DeMets *et al.* 1994) is magnetic anomaly data from the Gulf of California. Due to the rigid block motion of Baja California and incomplete coupling with the Pacific Plate, this rate must in reality represent North America–Baja California relative motion. When we compare our geodetic rate for North America–Baja California (46.8 ± 0.4 mm yr^{-1}) with the NUVEL-1A rate (47.4 ± 1.2 mm yr^{-1}) at the latitude of the spreading centre (23.5°N, 108.5°E) we see that these rates agree within uncertainties. On the other hand, when we compare at the same location our geodetic North America–Pacific rate (51.1 ± 0.4 mm yr^{-1}) with an estimate of DeMets (1995) that excludes the magnetic anomaly data from the Gulf of California and other problematic data sets from NUVEL-1A, his velocity (51.6 ± 1.9 mm yr^{-1}) agrees with our results (Fig. 7). This implies that the average spreading rate in the Gulf of California during the past 3 Myr is comparable to the geodetic rate over the last decade and the same is true for the rate of North America–Pacific Plate motion. We can exclude thermal contraction of the seafloor to be responsible for the velocity difference between Baja, and also Guadalupe, with respect to the stable Pacific Plate as the contraction can explain only ∼1.35 per cent of the spreading rate (Kumar *et al.* 2006), not the observed ∼10 per cent of difference.

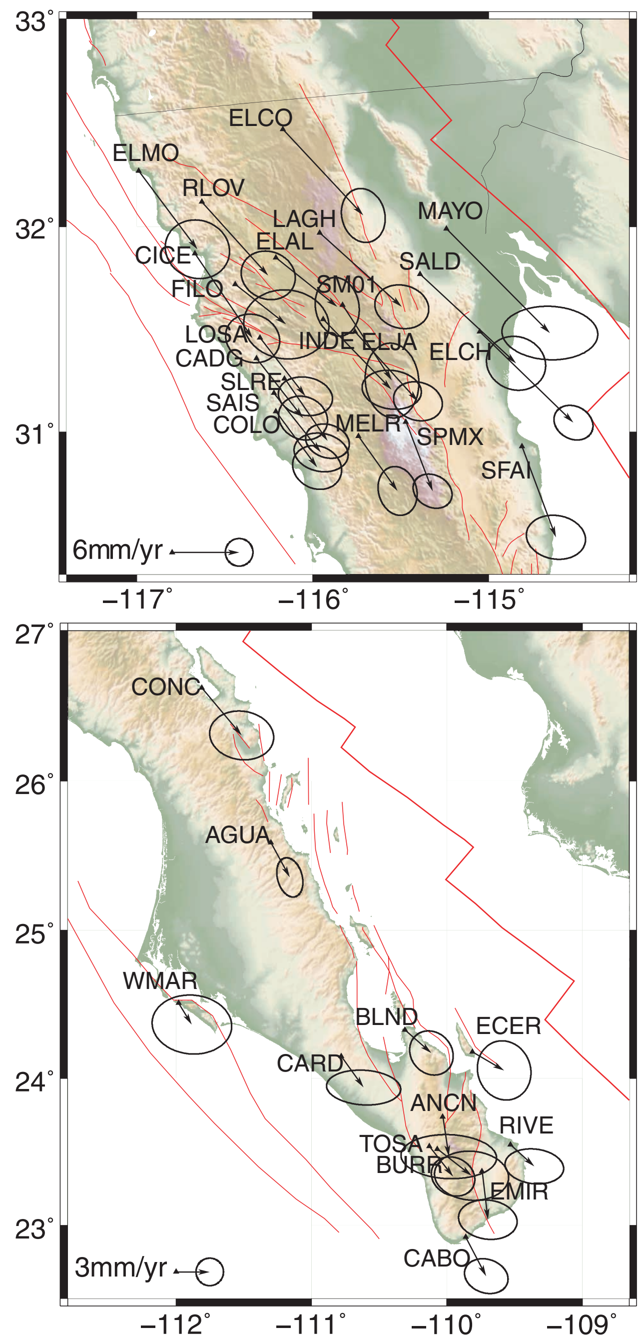

Figure 5. Northern (a) and southern (b) GPS network on Baja California: velocity with respect to stable Pacific Plate Euler vector 1 (Table 1). Error ellipses indicate 95 per cent confidence interval.

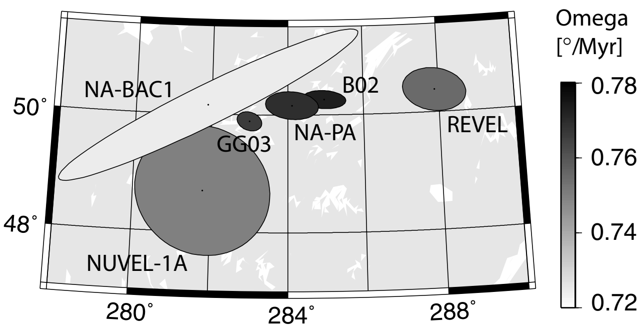

Figure 6. Location and magnitude of North America–Pacific (NA-PA) Euler vectors and North America–Baja California (NA-BAC1) Euler vector. If not otherwise indicated, results are from this study. NUVEL-1A (DeMets *et al*. 1994), Revel (Sella *et al*. 2002), B02 (Beavan *et al*. 2002) and GG03 (Gonzalez-Garcia *et al*. 2003). Ellipses show the 1σ error from a 2-D distribution.

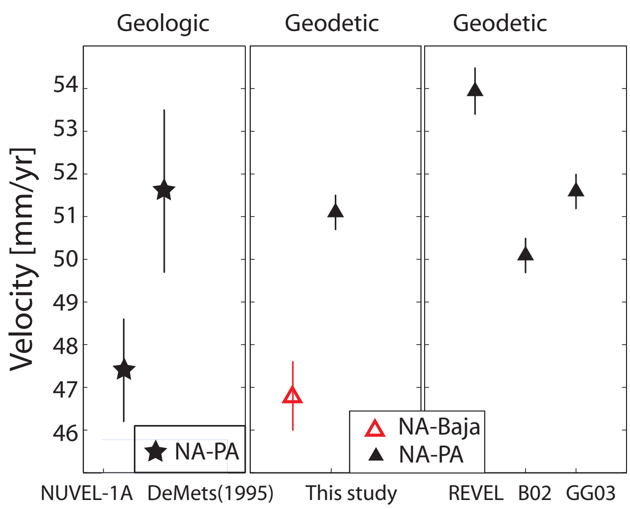

Figure 7. Magnitude of NA-PA and NA-Baja relative motion computed for a location at the spreading centre in the Gulf of California (23.5° N, 108.5° W). The geodetic rates of NA-PA from different studies (for abbreviations see Fig. 6) agree with each other and with the rate from geological model of DeMets (1995). Nuvel1A (DeMets *et al.* 1994) agrees with NA-Baja.

DISCUSSION

Baja California and its rigid block motion is an analogue for other terranes that are transported northwest with the Pacific Plate while interacting with North America (Atwater & Stock 1988; McQuarrie & Wernicke 2005). The essentially rigid behaviour of such a microplate on geodetic timescales preserves the coherence of a terrane during translation over geological timescales. The correspondence of terrane transport direction with the Pacific Plate motion is consistent with the idea that the Pacific Plate is the driving force for terrane transport in this region. The subducted extent of the oceanic microplates that were captured by the Pacific Plate (Nicholson *et al.* 1994; Stock & Lee 1994) may also be an important influence.

The direction of Pacific–North America and Baja California–North America motion is similar, but Baja California moves significantly slower. This result supports the suggestion of a western Baja California shear zone (Dixon *et al.* 2000b), and is consistent with observations of right-lateral offset on Quaternary faults, and seismicity along the southwestern coast of Baja California (Spencer & Normark 1979; Legg *et al.* 1991; Fletcher & Munguia 2000; Michaud *et al.* 2004).

A possible explanation for why the Baja California microplate is only partially coupled to the Pacific Plate and for activity along the western Baja California shear zone (Dixon *et al*. 2000b) is the collision of the northwestward moving microplate with North America along the Transverse Ranges and the big bend of the San Andreas fault. This impact may cause the microplate to shear off the Pacific Plate, along an inherited weak zone, the former Farallon–North American Plate boundary along the western coast of Baja California. In this case the shear zone may have formed from north to south. This may explain why the northern part of the Baja California microplate shows larger relative motion with respect to Pacific Plate than southern part. An alternative explanation for this observed pattern, also consistent with the idea of collision along the northern boundary, is internal deformation within the Baja California microplate.

ACKNOWLEDGMENTS

This research is partially supported by DFG. CP is partially supported by the international graduate school thesis within the Elitenetzwerk Bayern. RM received support from the BMBF, Germany. THD is partially supported by NSF grant OCE0505075. We are very grateful to the operators of the CGPS sites used in this study, including the South Pacific Sea Level and Climate Monitoring Program funded by the Australian Government Aid project operated by Geoscience Australia, the member institutions of IGS, the Western Pacific Integrated Network of GPS (WING) operated by the ERI, and SOPAC. Some of the EGPS data was collected by SCEC, in particular Javier Gonzalez Garcia and Duncan Agnew. We express our gratitude to all people that helped in the collection of the GPS data, in particular the technicians from CICESE. We are very thankful to Paul Umhoefer for providing fault map data, and to Kevin Furlong, Jim Ray, and the reviewers Chuck DeMets and Joann Stock, whose comments helped to improve this paper.

REFERENCES

Argus, D.F. & Heflin, M.B., 1995. Plate motion and crustal deformation estimated with geodetic data from the Global Positioning System, *Geophys. Res. Lett.,* **22,** 1973–1976.

Atwater, T. & Stock, J., 1988. Pacific–North America Plate tectonics of the neogene Southwestern United States—an update, in *Integrated Earth and Environmental Evolution of the Southwestern United States: The Clarence A. Hall, Jr. Volume,* pp. 393–420, eds Ernst, W.G. & Nelson, C.A., Bellwether Publishing, Columbia.

Beavan, J., Tregoning, P., Bevis, M., Kato, T. & Meertens, C., 2002. Motion and rigidity of the Pacific Plate and implications for plate boundary deformations, *J. Geophys. Res.,* **107,** 2261, doi:10.1029/2001JB000282.

Busch, M. *et al.* 2006. Late Quaternary faulting in the Cabo San Lucas-La Paz Region, Baja California, *Eos Trans. AGU,* **87**(52), Fall Meet. Supol., Abstract T41D-1612.

DeMets, C., 1995. A reappraisal of seafloor spreading lineations in the Gulf of California: implications for the transfer of Baja California to the Pacific plate and estimates of Pacific-North America motion, *Geophys. Res. Lett.,* **22,** 3545–3548.

DeMets, C. & Dixon, T.H., 1999. New kinematic models for Pacific-North America motion from 3 Ma to present, I: evidence for steady motion and biases in the NUVEL-1A model, *Geophys. Res. Lett.,* **26,** 1921–1924.

DeMets, C., Gordon, R.G., Argus, D.F. & Stein, S., 1990. Current plate motions, *Geophys. J. Int.,* **101,** 425–478.

DeMets, C., Gordon, R.G., Argus, D.F. & Stein, S., 1994. Effect of recent revisions to the geomagnetic reversal time-scale on estimates of current plate motions, *Geophys. Res. Lett.,* **21,** 2191.

Dixon, T.H., Miller, M., Farina, F., Wang, H. & Johnson, D., 2000a. Present day motion of the Sierra Nevada block and some implications for the Basin and Range province, North America Cordillera, *Tectonics,* **19,** 1–24.

Dixon, T.H. *et al.* 2000b. New kinematics for Pacific-North America motion from 3 Ma to present, II: evidence for a "Baja California shear zone", *Geophys. Res. Lett.,* **27,** 3961–3964.

Dixon, T.H. *et al*. 2002. Seismic cycle and rheological effects on estimation of present-day slip rates for the Agua Blanca and San Miguel-Vallecitos faults, northern Baja California, Mexico, *J. Geophys. Res.,* **107,** doi:10.1029/2000JB000099.

Fletcher, J.M. & Munguia, L., 2000. Active continental rifting in southern Baja California, Mexico: implications for plate motion partitioning and the transition to seafloor spreading in the Gulf of California, *Tectonics,* **19,** 1107–1123.

Freymueller, J.T., Murray, M.H., Segall, P. & Castillo, D., 1999. Kinematics of the Pacific–North America plate boundary zone, northern California, *J. Geophys. Res.,* **104,** 7419–7441.

Gastil, R.G., Phillips, P.R. & Allison, C.E., 1975. Reconnaissance Geology of the State of Baja California, *Geol. Soc. Am. Mem.,* **140,** 170 p.

Gonzales-Garcia, J.J., Prawirodirdjo, L., Bock, Y. & Agnew, D., 2003. Guadalupe Island, Mexico as a new constraint for Pacific plate motion, *Geophys. Res. Lett.,* **30**(16), 1872, doi:10.1029/2003GL017732.

Govers, R. & Wortel, M.-J.-R., 2005. Lithosphere tearing at STEP faults: response to edges of subduction zones, *Earth Plant. Sc. Lett.,* **236**(1–2), 505–523.

Hausback, B.P., 1984. Cenozoic volcanic and tectonic evolution of Baja California Sur, Mexico, in Geology of the Baja Peninsula, Frizell, V.A. (ed.), *Pac. Sect. Soc. of Econ. Paleontol. and Mineral.*, Vol. **39**. pp. 219–236, Los Angeles, CA.

Kumar, R.R., Gordon, R.G. & Landis, C.M., 2006. Horizontal thermal contractional strain of oceanic lithosphere: the ulimate limit to the rigid plate hypothesis, *Eos Trans. AGU,* **87**(52), Fall Meet. Suppl., Abstract G41A-04.

Lachenbruch, A.H., Sass, J.H., & Galanis, S.P., Jr., 1985. Heat flow in southernmost California and the origin of the Salton trough, *J. Geophys. Res.,* **90,** 6709–6736.

Larson, K.M., Freymueller, J.T. & Philipsen, S., 1997. Global plate velocities from the Global Positioning System, *J. Geophys. Res.,* **102,** 9962–9982.

Legg, M.R., Wong, V.O. & Suarez-Vidal, F., 1991. Geologic structure and tectonics of the inner continental borderland of northern Baja California, in *Gulf and Peninsular Province of the Californias*, Vol.47, pp. 145–177, eds J. Dauphin & B. Simoneit, *Am. Assoc. Pet. Geol. Mem.*.

Mao, A., Harrison, G.A. & Dixon, T.H., 1999. Noise in GPS coordinate time series, *J. Geophys. Res.,* **104,** 2797–2816.

McCaffrey, R., 2002. Crustal block rotations and plate coupling, in *Plate Boundary Zones, Geodyn. Ser.,* Vol. 30, pp. 101–122, eds S. Stein & J. Freymueller.

McQuarrie, N. & Wernicke, B.P., 2005. An animated tectonic reconstruction of southwestern North America since 36 Ma. *Geosphere,* **1**(3), doi: 10.1130/GES00016.1, 147–172.

Michaud F. et al. 2004. Motion partitioning between the Pacific plate, Baja California and the North America plate: the Tosco-Abreojos fault revisited, *Geophys. Res. Lett.,* **31,** L08604, doi:10.1029/2004GL019665.

Minster, J.B., Jordon, T.H., Molnar, P. & Haines, E., 1974. Numerical modelling of instantaneous plate tectonics, *Geophys. J. R. astr. Soc.,* **36,** 541–576.

Nicholson, C., Sorlien, C.C., Atwater, T., Crowell, J.C. & Luyendyk, B.P., 1994. Microplate capture, rotation of the western Transverse Ranges, and initiation of the San Andreas transform as a low-angle fault system, *Geology,* **22,** 491–195.

Ray, J., Dong, D. & Altamimi, Z., 2004. IGS reference frames: status and future improvements, *GPS Solutions,* **8,** 251–266.

Sella, G.F., Stein, S., Dixon, T.H., Craymer, M., James, T.S., Mazzotti, S. & Dokka, R.K., 2006. Observation of glacial isostatic adjustment in "stable" North America with GPS, *Geophy. Res. Lett.,* **34,** L02306, doi: 10.1029/2006GL027081.

Sella, G.F., Dixon, T.H. & Mao, A.L., 2002. REVEL: a model for Recent plate velocities from space geodesy, *J. Geophys. Res.,* **107,** doi:10.1029/2000JB000033.

Spencer, J.-E. & Normark, W., 1979. Tosco-Abreojos fault zone: a neogene transform plate boundary within the Pacific margin of southern Baja California, Mexico, *Geology,* **7,** 554–557.

Stein, S. & Gordon, R.G., 1984. Statistical tests of additional plate boundaries from plate motion inversions, *Earth Plan. Sci. Lett.,* **69**(2), 401–412.

Stock, J. M. & J. Lee, 1994. Do microplates in subduction zones leave a geological record? *Tectonics,* **13**(6), 1472–1487, doi: 10.1029/94TC01808.

Suarez-Vidal, F., Armijo, R., Morgan, G., Bodin, P. & Gastil, R.G., 1991. Framework of recent and active faulting in Northern Baja California, in *Gulf and Peninsular Province of the Californias*, Vol.47, pp. 285–300, eds J. Dauphin & B. Simoneit, *Am. Assoc. Pet. Geol. Mem*.

Umhoefer, P.J., 2000. Where are the missing faults in translated terranes?, *Tectonophysics,* **326,** 23–35.

Umhoefer, P.J. & Dorsey, R.J., 1997. Translation of terranes; lessons from central Baja California, Mexico, *Geology,* **25,** 1007–1010.

Ward, S., 1990. Pacific-North America Plate motions: new results from very long baseline interferometry, *J. Geophys. Res.,* **95,** 21 965–21 981.

Zumberge, J.F., Heflin, M.B., Jefferson, D.J., Watkins, M.M. & Webb, F.H., 1997. Precise point positioning for the efficient and robust analysis of GPS data from large networks, *J. Geophys. Res.,* **102,** 5005–5017.